

Synthesis and triplex forming properties of pyrrolidino pseudoisocytidine containing oligodeoxynucleotides

Alain Mayer, Adrian Häberli and Christian J. Leumann*

Department of Chemistry & Biochemistry, University of Berne, Freiestrasse 3, CH-3012, Berne, Switzerland. E-mail: leumann@ioc.unibe.ch; Fax: +41(0)31 631 3422; Tel: +41(0)31 631 4355

Received 24th February 2005, Accepted 21st March 2005

First published as an Advance Article on the web 7th April 2005

Pyrrolidino pseudo-*C*-nucleosides are isosteres of natural deoxynucleosides which are protonated at the pyrrolidino ring nitrogen under physiological conditions. As constituents of a triplex forming oligodeoxynucleotide (TFO), the positive charge is expected to stabilise DNA triple helices *via* electrostatic interactions with the phosphodiester backbone of the target DNA. We describe the synthesis of the pyrrolidino isocytidine pseudonucleoside and the corresponding phosphoramidite building block and its incorporation into TFOs. Such TFOs show substantially increased DNA affinity compared to unmodified oligodeoxynucleotides. The increase in affinity is shown to be due to the positive charge at the pyrrolidino subunit.

Introduction

Sequence specific binding of triplex forming oligonucleotides (TFOs) in the major groove of double stranded DNA can control and modulate gene expression at the level of transcription and is the basis of antigene technology.¹ TFOs can bind to homopurine/homopyrimidine tracts of DNA in either parallel or antiparallel alignment relative to the purine target strand, forming Hoogsteen or reversed-Hoogsteen base-triples. Unfortunately, the use of triplex forming oligonucleotides (TFOs) as antigene agents suffers from several limitations. Low thermal stability of the triplexes, low biostability of the TFOs *in vivo*, low bioavailability, sequence restrictions to homopurine/homopyrimidine DNA tracts and a strong pH dependence in the parallel binding motif due to C⁺·G–C triplet formation are among the major disadvantages that reduce the efficacy of antigene agents and that slow down the development and applications of antigene technology. Many strategies have been exploited to avoid these drawbacks,² including the use of conformationally restricted DNA analogues to increase thermal stability³ and the design of new selective nucleobase analogues to alleviate target sequence restriction.⁴

As part of our current research we are interested in increasing TFO affinity to a DNA target by applying the ‘dual recognition’ approach, originally developed by Cuenoud and coworkers.⁵ In this approach, a target dsDNA is not only recognised by selective base–base interactions but also *via* an additional, non-specific salt bridge between an appropriately placed positive charge in the TFO and a negatively charged phosphate oxygen in the target DNA backbone.

Based on a recent X-ray data on a parallel DNA triplex,⁶ molecular modelling showed that replacement of the 4'-oxygen in a deoxynucleoside residue of a TFO by a basic nitrogen would potentially place a positive charge next to a non-bridging pro-*R*-phosphate oxygen of the purine strand of a target dsDNA (Fig. 1). In recent studies we explored pyrrolidino pseudonucleosides containing the base uracil (dpψU) and *N*-1-methyl uracil (dpψT, Fig. 1) for A–T base-pair recognition.^{7,8} Analysis of corresponding TFOs showed a destabilisation relative to thymidine in a sequence dependent manner. Interestingly, duplex formation was only marginally destabilised and the sequence effects were less pronounced.

In order to complement this study we focused now on the pyrrolidino analogue of pseudoisocytidine in order to recognise target G–C base-pairs.⁹ Here we report on the synthesis of pyrrolidino pseudoisocytidine (dpψiC, Fig. 1) *via* Heck chemistry and its incorporation into oligodeoxynucleotides. The triplex

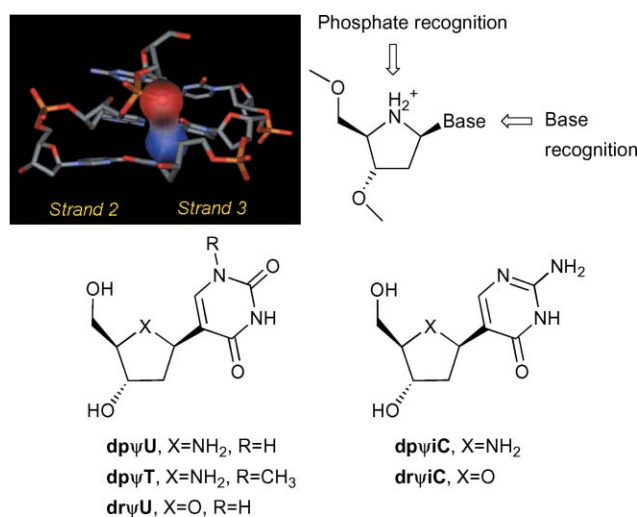


Fig. 1 Top: ‘dual recognition’ principle for pyrrolidino pseudonucleosides (strand 2 corresponds to the purine strand and strand 3 to the TFO in a modeled triplex); bottom: pyrrolidino pseudonucleoside analogues of deoxyuridine (dpψU), thymidine (dpψT) and deoxycytidine (dpψiC) as well as their deoxyribo-equivalents used for comparison.

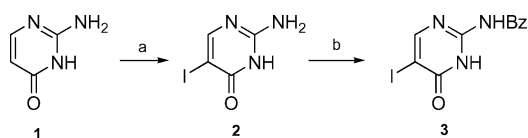
forming properties of TFOs containing dpψU(T) and dpψiC were evaluated using UV melting curve analysis, CD spectroscopy and gel mobility shift experiments. For comparison, 2'-deoxypseudoisocytidine (drψiC) and 2'-deoxypseudouridine (drψU) containing TFOs in the same sequence context were studied as well, allowing for an analysis of the contribution of the pyrrolidino modification. For this we recently also developed a convenient synthesis of the drψiC phosphoramidite building block.¹⁰

Results and discussion

Synthesis of the monomer

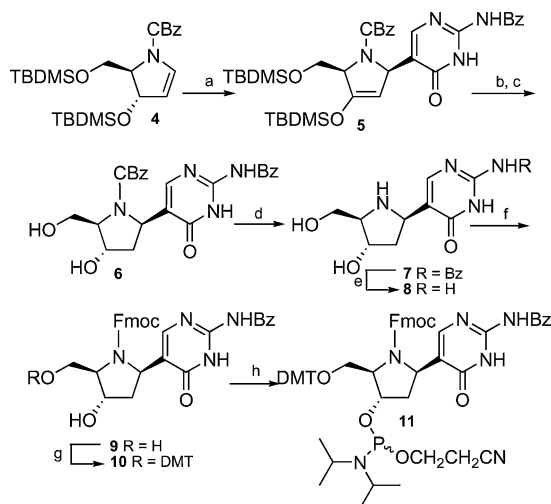
We based our synthesis of the dpψiC monomer **8** on a palladium catalysed Heck reaction as already applied successfully for the synthesis of the dpψU and dpψT monomers.⁷ As precursors, we envisioned the CBz protected enamine **4** and the corresponding protected iodoisocytosine **3**. Enamine **4** could be obtained in seven steps and 52% overall yield starting from *trans*-3-hydroxy-L-proline.⁷ The necessary 2-*N*-benzoyl-5-iodoisocytosine (**3**) was prepared in two steps from commercially available isocytosine **1**

via iodination with NIS in AcOH, followed by benzylation of the exocyclic amino function under standard conditions in good yield (Scheme 1).



Scheme 1 Reagents and conditions: (a) NIS, AcOH, 70 °C → 100 °C, 1 h, 87%; (b) benzoic anhydride, DMF, 100 °C, 1.5 h, 76%.

The palladium catalyzed Heck reaction of enamine **4** with base **3** using Pd(OAc)₂ as catalyst, AsPh₃ as a soft ligand and diisopropylethylamine as base gave selectively the β-pyrrolidino derivative **5** in 63% yield (Scheme 2). *In situ* silylation of **3** with BSA was necessary due to its poor solubility in DMF. The β-configuration at the pseudo anomeric centre was spectroscopically confirmed at a later stage. After removal of the silyl protecting groups with HF-pyridine in acetonitrile, the resulting ketone was diastereoselectively reduced with NaBH(OAc)₃ to yield diol **6**. The cleavage of the CBz group (**6** → **7**) was then accomplished by catalytic hydrogenation. A sample of compound **7** was converted (conc. NH₃) to the fully deprotected nucleoside **8** for spectroscopic analysis. The relative configurations at C(1') and C(3') (nucleoside numbering scheme) in **8** could unambiguously be assigned by ¹H-NMR-NOE experiments (see Experimental).



Scheme 2 Reagents and conditions: (a) i) **3**, BSA, DMF, rt, 1 h; ii) **4**, *i*Pr₂NEt, Pd(OAc)₂, AsPh₃, DMF, 80 °C, 22 h, 63%; (b) HF-pyridine, MeCN, rt, 6 h; (c) NaBH(OAc)₃, AcOH, MeCN, -15 °C → rt, 5 h, 79%; (d) H₂, Pd/C, MeOH, rt, 7 h, 99%; (e) conc. NH₃, 55 °C, 18 h, 83%; (f) Fmoc-OSu, THF, dioxane, 5% aq. NaHCO₃, rt, 3 h; (g) DMT-Cl, pyridine, rt, 2 h, 47%; (h) (*i*Pr₂N)(NCCH₂CH₂O)PCI, *i*Pr₂NEt, THF, rt, 2 h, 88%.

The pyrrolidino ring nitrogen in **7** was then Fmoc protected (→ **9**), as this base labile protecting group is compatible with the regular protecting group scheme in oligodeoxynucleotide

synthesis. The hardly soluble product **9** was subsequently subjected to dimethoxy-tritylation (→ **10**), followed by standard phosphorylation to yield the phosphoramidite building block **11** in 17% overall yield from **4**.

Synthesis of oligodeoxynucleotides

Oligodeoxynucleotides were synthesised on a 1.0 or 1.3 μmol scale on a DNA synthesiser using standard solid-phase phosphoramidite chemistry. Minor modifications to the synthesis cycle were introduced for the incorporation of the non-natural building blocks. More precisely, the coupling time was extended from 1.5 to 6 min and the standard activator tetrazole was replaced by the more powerful (*S*-benzylthio)-1*H*-tetrazole. Coupling efficiencies for the modified units were typically >97%, according to trityl assay. Standard ammonia deprotection led to cleavage of the crude oligonucleotides from the solid support and removal of all protecting groups (including Fmoc). Crude oligomers were purified by ion exchange HPLC and characterised by ESI-mass spectrometry. A summary of the modified oligomers synthesised and their mass spectrometric analysis is provided in Table 1. The triplex forming properties of the modified oligodeoxynucleotides were subsequently examined by UV melting curve analysis, CD spectroscopy and gel electrophoresis.

Pairing properties with DNA duplexes in the parallel motif

The *T_m* of TFO dissociation from a 21-mer dsDNA target are summarized in Table 2. Since protonation of the pyrrolidino ring nitrogen is pH-dependent, the melting experiments were carried out at different pH values. NMR titration experiments with the monomer dpψU revealed a p*K_a* of 7.9.⁸ Therefore we chose to investigate triplex formation in the pH range from 6 to 9.

At pH 6, where the pyrrolidino ring nitrogen is fully protonated, the triplexes with TFOs **dp1**–**3**, bearing dpψiC residues (Table 2), were more stable than the one formed with the reference TFO **Ref1**, in which the modified units were replaced by deoxycytidine. Each modification contributed to triplex stability by 1.9 to 2.4 °C. The most stable of all investigated triplexes was found to be **dp3** with five dpψiC units and a *T_m* that was ca. 10 °C higher than that of the corresponding unmodified triplex. The TFOs **dr1**–**3**, containing pseudoisocytidine units (Table 2), were used to identify affinity differences arising exclusively from the change of the nucleobase. We found a decrease in *T_m* per mod. by ca. 2.5–5.0 °C for these TFOs, relative to the DNA control **Ref1**. This clearly shows that the pyrrolidino modification is contributing significantly to stability, as it is able to overcompensate for the generally destabilising nature of the pseudobases under the given conditions.

Of special interest was TFO **dp3** in which all deoxycytidines were replaced by dpψiC units. In contrast to deoxycytidine, the isocytidine pseudonucleosides need no protonation at the bases upon binding to their target G–C base-pairs. Thus, any dependence of target binding of **dp3** from pH in the interval of pH 6–9 must be due to a change of the protonation state of the pyrrolidino ring nitrogen. Indeed, raising the pH from 6.0 to 9.0 leads to a reduction in triplex *T_m* by 25 °C, corresponding to 3 °C per mod. In contrast, and as expected, **dr3**, containing deoxypseudoisocytidine residues instead of the pyrrolidino

Table 1 Sequence and ESI-MS data of the modified oligonucleotides investigated in this study

| TFO | Sequence | Mod. | [M–H] [–] (calcd) | [M–H] [–] (found) |
|------------|----------------------|---------------------|----------------------------|----------------------------|
| dp1 | 5'-d(TTTTCTXTCTCTCT) | X = dpψiC | 4423.9 | 4424.4 |
| dr1 | 5'-d(TTTTCTXTCTCTCT) | X = drψiC | 4424.9 | 4424.7 |
| dp2 | 5'-d(TTTTXTCTXTCTCT) | X = dpψiC | 4422.9 | 4423.6 |
| dr2 | 5'-d(TTTTCTXTCTCTCT) | X = drψiC | 4424.9 | 4424.8 |
| dp3 | 5'-d(TTTTXTXTXTXTXT) | X = dpψiC | 4419.8 | 4420.3 |
| dr3 | 5'-d(TTTTXTXTXTXTXT) | X = drψiC | 4424.9 | 4424.8 |
| dp4 | 5'-d(YYYYYYXYXYXYXT) | X = dpψiC, Y = dpψU | 4284.9 | 4285.0 |
| dp5 | 5'-d(TTXXXXTTTXXXXT) | X = dpψiC | 4420.0 | 4420.3 |
| dr5 | 5'-d(TTXXXXTTTXXXXT) | X = drψiC | 4424.9 | 4425.0 |

Table 2 T_m data ($^{\circ}\text{C}$) of third strand dissociation from UV melting curves (260 nm)

| Target | 5'-d(GCTAAAAAGAGAGAGATCG) 3'-d(CGATTTTTCTCTCTCTAGC) | | |
|--------------------------|---|-------------------|--------------------------|
| TFO | pH | T_m^a | $\Delta T_m/\text{mod.}$ |
| Ref1 ^b | 6.0 | 43.1 | 0 |
| dp1 | 6.0 | 45.5 | +2.4 |
| dr1 | 6.0 | 39.9 | -3.2 |
| dp2 | 6.0 | 46.9 | +1.9 |
| dr2 | 6.0 | 37.9 | -2.6 |
| dp3 | 6.0 | 53.0 | +2.0 |
| | 7.0 | 44.4 | - |
| | 8.0 | 37.1 | - |
| | 9.0 | 28.0 | - |
| dr3 | 6.0 | 16.4 | -5.3 |
| | 7.0 | 11.2 | - |
| | 8.0 | 13.5 | - |
| | 9.0 | 10.0 | - |
| dp4 | 6.0 | n.d. ^c | n.d. ^c |

^a Single strand concentration = 1.2 μM in 140 mM KCl, 7 mM NaH_2PO_4 , 0.5 mM MgCl_2 . T_m of target duplex = $57.0 \pm 1.0^{\circ}\text{C}$. ^b **Ref1** = 5'-d(TTTTCTCTCTCT). ^c No T_m detectable.

pseudoisocytidines, essentially shows no pH dependence in target binding, indicating that no reversible protonation events are involved in target binding.

These results unambiguously highlight the importance of the protonated state of the pyrrolidino units in target binding and are in agreement with the 'dual recognition' principle by specific base-base interactions and unspecific salt bridge formation between the protonated pyrrolidino nitrogens of the TFO and phosphate units of the target DNA.

The fully modified $\text{dp}\psi\text{U}$ and $\text{dp}\psi\text{iC}$ containing TFO **dp4** (Table 2) did not show any triplex formation with its target. The observed monophasic UV-melting transition could be attributed to the melting of the Watson-Crick duplex. This result is in line with earlier observations with TFOs containing only $\text{dp}\psi\text{U}$ units that were found to strongly destabilise triplexes.⁸ Obviously the destabilising effect of the nine $\text{dp}\psi\text{U}$ units cannot be compensated by the five $\text{dp}\psi\text{iC}$ units in **dp4**.

In order to test for sequence effects, a different sequence context was explored. The corresponding modified 15-mer TFOs, their DNA target and the T_m values for third strand melting at pH values between 6 and 8 are summarized in Table 3. These data were again compared with those of the reference TFO **Ref2** bearing 5-methyldeoxycytidine (^{Me}C) instead of deoxycytidine at the X-positions.

At pH 6 the oligonucleotide **dp5**, containing five $\text{dp}\psi\text{iC}$ units, binds to the target duplex with considerably higher affinity than the reference TFO **Ref2**. The T_m is *ca.* 13 $^{\circ}\text{C}$ higher and the ΔT_m per mod. of 2.6 $^{\circ}\text{C}$ is of the same order as in the previous sequence context. Again, the T_m drop upon increasing the pH from 6–8 due to partial deprotonation of the pyrrolidino nitrogen. Remarkably, even at pH 8 where **Ref2** has no detectable affinity to its target, **dp5** still binds dsDNA with a T_m of *ca.*

Table 3 T_m data ($^{\circ}\text{C}$) of third strand dissociation from UV melting curves (260 nm)

| Target | 5'-d(GCTAAAGGGGAAAAGAAATCG) 3'-d(CGATTTCCCCTTTTCTTAGC) | | |
|--------------------------|--|-------------------|--------------------------|
| TFO | pH | T_m^a | $\Delta T_m/\text{mod.}$ |
| Ref2 ^b | 6 | 27.2 | 0 |
| | 7 | n.d. ^c | 0 ^c |
| | 8 | n.d. ^c | 0 ^c |
| dp5 | 6 | 40.0 | +2.6 |
| | 7 | 36.2 | - |
| | 8 | 29.3 | - |
| dr5 | 6 | 16.5 | -2.1 |
| | 7 | 11.8 | - |
| | 8 | 11.0 | - |

^a Single strand concentration = 1.2 μM in 140 mM KCl, 7 mM NaH_2PO_4 , 0.5 mM MgCl_2 . T_m of target duplex = $60.0 \pm 1.0^{\circ}\text{C}$. ^b **Ref2** = 5'-d(TTCCCCTTTTCTTT), C = ^{Me}C. ^c No T_m detectable.

30 $^{\circ}\text{C}$. This T_m is even higher than that of **Ref2** at pH 6. The TFO **dr5**, containing five $\text{dr}\psi\text{iC}$ units, was again used for dissecting the role of the sugar modification. As expected, the T_m s between pH 6.0 and 8.0 are similar ruling out protonation events upon target binding. In addition, their values between 11–16 $^{\circ}\text{C}$ are considerably lower than that of **dp5**, again demonstrating the superiority of the $\text{dp}\psi\text{iC}$ units.

To confirm the negative binding result of the fully modified **dp4** (where only one transition was observed in the UV melting curve) and to corroborate the positive results obtained for the $\text{dp}\psi\text{iC}$ containing TFOs **dp3** and **dp5**, a gel retardation experiment was performed (Fig. 2).

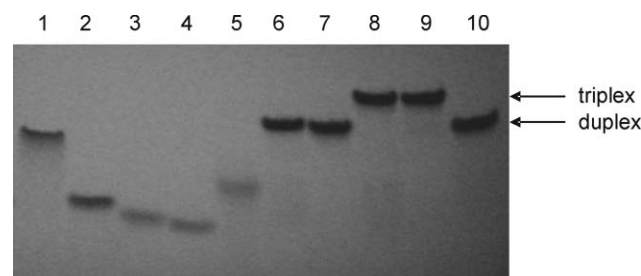


Fig. 2 UV shadowing of a non-denaturing 20% polyacrylamide gel at pH 7.1. Lanes 1 and 2: purine rich and pyrimidine rich single strands of the DNA target for **dp3** and **dp4**; lane 3–5: **dp3**, **dp5** and **dp4** (single strands); lane 6 and 7: target duplexes; lane 8: ternary mixture of **dp5** with its target duplex strands; lane 9: ternary mixture of **dp3** with its target duplex strands; lane 10: ternary mixture of **dp4** with its target duplex strands. 0.7 nmol of each strand was used with equal stoichiometry in mixtures.

From the ternary mixtures of the TFOs **dp3**, **dp5** and **dp4** with their duplex targets, it clearly emerges that no triplex is formed in the latter case (lane 10) while stable triplexes occur in the two former cases (lane 8 and 9).

In order to get additional information on target binding by $\text{dp}\psi\text{C}$ containing TFOs, the triplex involving **dp3** was analyzed by CD spectroscopy. The CD spectra were measured at different temperatures below and above the T_m of the third strand (Fig. 3, top). The resulting curves were almost identical in shape, except in the region below 235 nm. At low temperature, the curves show a minimum around 220 nm, characteristic of a triple helical structure, which evolves into a maximum upon raising the temperature to above 50 °C. This change coincides with the melting of the triplex to the duplex. Consequently a CD melting curve at a fixed wavelength of 217 nm was recorded (Fig. 3, bottom). As in the UV melting experiments, a heating-cooling-heating cycle was applied and sigmoidal curves were obtained. The two heating ramps were superimposable while the cooling ramp showed slight hysteresis. A T_m value of 48 °C was determined which is in agreement with that from the UV-melting results.

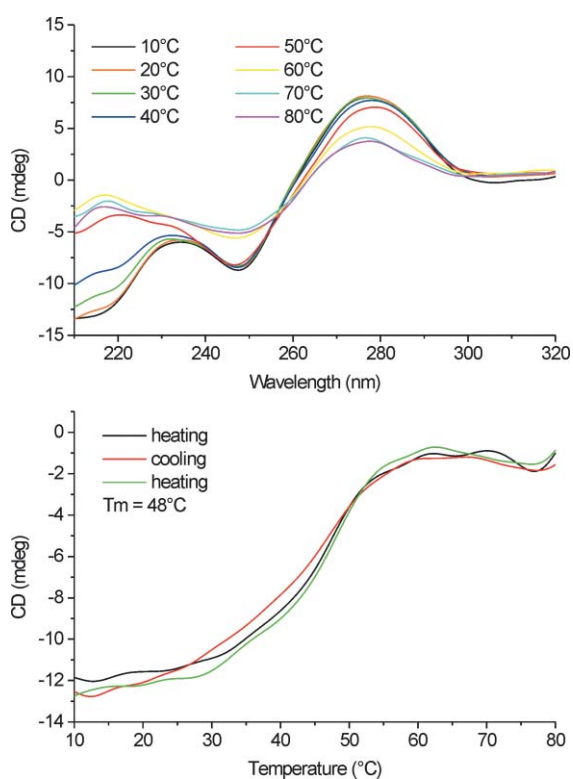


Fig. 3 CD spectra of the triplex containing TFO **dp3**; top: CD spectra measured at various temperatures; bottom: temperature scan CD spectra from 10 to 80 °C at 217 nm; single strand concentration = 1.2 μM in 140 mM KCl, 7 mM NaH_2PO_4 , 0.5 mM MgCl_2 , pH 6.0.

Conclusions

Introduction of positive charges at strategic positions within a TFO has proven in the past to be a valuable tool to improve triplex stability by favourable additional electrostatic interactions with the negatively charged phosphodiester backbone of the target duplex. Most of the strategies developed so far were based on the attachment of corresponding chemical functions at various positions of the sugar,^{5a-c} the base¹¹ or the phosphate backbone.¹² The pyrrolidino pseudonucleoside $\text{dp}\psi\text{C}$, as reported here, is a valuable extension of the ‘dual recognition’ concept and provides a novel molecular platform.

TFOs containing pyrrolidino pseudoisocytidine units ($\text{dp}\psi\text{C}$ -series) exhibit a significant increase in triplex stability compared to unmodified TFOs in at least two different sequence

contexts. By comparison with TFOs containing ribo-pseudo- iC units ($\text{dr}\psi\text{C}$ -series), it clearly emerges that the increase in stability is associated with the protonation of the pyrrolidino ring nitrogen which confirms the presence of attractive electrostatic interactions between the additional positive charge in the TFOs and the phosphodiester backbone of the target duplex.

A puzzling situation remains in that this additional electrostatic stabilisation seems to be restricted to $\text{dp}\psi\text{C}$ units and does not occur with $\text{dp}\psi\text{U}$ units, as reported earlier (see also binding properties of **dp4**).⁸ In the case of the $\text{dp}\psi\text{U}$ and its *N*-1-methyl derivative, the pyrrolidino modification was shown to destabilise a triplex, while in the case of $\text{dp}\psi\text{C}$ the pyrrolidino unit significantly stabilises the triplex. On the basis of a X-ray triplex structure we found that *O*-(4′)-*pro-R*-phosphate oxygen distances vary between 3.4–4.0 Å from base-triple to base-triple.⁶ Given the fact that electrostatic interactions are strongly distance dependent, it is possible that local structural variations in the N–O distances (sequence effects) might account for the differential stability. Another reason might be a generally unfavourable TFO conformation of oligodeoxyribonucleotides for dual recognition (B- vs. A-conformation). Indeed, dual recognition of sugar modified TFOs was so far only found to be effective for those preferring A helix conformations (e.g. the 2′-aminoethyl nucleosides). It might therefore be of interest to study RNA-TFOs containing single $\text{dp}\psi$ -modifications or the corresponding pyrrolidino pseudonucleosides with a 2′-hydroxyl function in the ribo-configuration.

Experimental

General

Solvents for chromatography and extraction were distilled prior to use. Chemicals for synthesis were generally reagent grade. All moisture sensitive reactions were performed in oven dried glassware in anhydrous solvents under an Ar atmosphere. External bath temperatures were used to record all reaction temperatures. Spectral data (NMR, MS) were measured with standard equipment and are indicated in standard format. J values are given in Hz and chemical shifts were referenced to the residual, non-deuterated solvent used. Multiplicity assignments for ^{13}C -signals were from DEPT spectra. Flash chromatography (FC) was performed using silica gel 60 (230–400 mesh). Thin-layer chromatography (TLC) was performed on pre-coated silica gel plates SIL-G-25 UV₂₅₄ (Macherey-Nagel).

2-Amino-5-iodo-4-oxo-3,4-dihydropyrimidine 2. To a solution of 2-amino-4-oxo-3,4-dihydropyrimidine **1** (5.20 g, 46.8 mmol) in AcOH (84 cm³) at 70 °C was added *N*-iodosuccinimide (11.6 g, 51.6 mmol) and the suspension was heated to 100 °C. After 1 h, the mixture was cooled to rt and H₂O (84 cm³) was added. The solid was filtered over a filter paper (Whatman 1PS), washed with H₂O and dried under HV to give **2** (9.68 g, 87%) as a white solid. Mp 245–250 °C (decomp.). δ_{H} (300 MHz; $(\text{CD}_3)_2\text{SO}$) 6.70 (2 H, br s, NH₂), 7.93 (1 H, s, C(6)H), 11.26 (1 H, br s, NH); δ_{C} (75 MHz; $(\text{CD}_3)_2\text{SO}$) 71.3 (s, C(5)), 156.8 (d, C(6)), 160.0, 161.4 (2 × s, C(2, 4)); m/z (FAB⁺) 237.9497 (M^+ + H. C₄H₅N₃OI requires 237.9477).

2-(*N*-Benzoylamino)-5-iodo-4-oxo-3,4-dihydropyrimidine 3. A suspension of **2** (5.00 g, 21.1 mmol) and benzoic anhydride (12.6 g, 55.7 mmol) in dry DMF (80 cm³) was heated to 100 °C. After 1.5 h, a clear, slightly yellow solution was obtained. Most of the DMF was evaporated and the residue suspended in EtOH (150 cm³). The solid was filtered off (Whatman 1PS) and washed with cold EtOH (150 ml). Drying under HV afforded dihydropyrimidine **3** (5.46 g, 76%) as a white powder. Mp 296–299 °C (decomp.). δ_{H} (300 MHz; $(\text{CD}_3)_2\text{SO}$) 7.54 (2 H, t, J 7.5, Bz), 7.67 (1 H, t, J 7.4, Bz), 8.03 (2 H, d, J 7.4, Bz), 8.31 (1 H, s, C(6)H), 12.25 (2 H, br s, 2 × NH); δ_{C} (75 MHz; $(\text{CD}_3)_2\text{SO}$) 81.2 (s, C(5)), 128.7 (d, Bz), 132.6 (s, Bz),

133.36 (d, Bz), 152.5 (d, C(6)), 159.0, 160.7 (2 × s, C(2, 4)), 169.8 (s, C=O); *m/z* (FAB⁺) 341.9752 (M⁺ + H. C₁₁H₉N₃O₂I requires 341.9739).

(2R,5R)-N-(Benzyloxy)carbonyl-2-[2-(N-benzoylamino)-4-oxo-3,4-dihydropyrimidin-5-yl]-4-(tert-butyl)dimethylsilyloxy-5-(tert-butyl)dimethylsilyloxymethyl-aza-cyclopent-3-ene 5. To a suspension of **3** (2.73 g, 8.00 mmol) in dry DMF (16 cm³) was added dropwise *N,O*-bis(trimethylsilyl)acetamide (BSA, 2.45 cm³, 10.0 mmol). After 1 h, *N,N*-diisopropylethylamine (1.87 cm³, 10.9 mmol) and pyrrolidine **4** (1.60 g, 3.34 mmol) were added to the clear solution. To a separate solution of triphenylarsine (408 mg, 1.33 mmol) in dry DMF (48 cm³) was added Pd(OAc)₂ (150 mg, 0.67 mmol). After 30 min, this solution was added dropwise to the first solution and the mixture was heated at 80 °C for 22 h. The reaction was quenched by the addition of H₂O (20 cm³) and most of the solvents were evaporated. The residue was diluted with EtOAc, washed with H₂O, the organic phase dried (MgSO₄) and evaporated. FC (toluene–THF 7 : 1 → 4 : 1 + 0.1% NEt₃) afforded compound **5** (1.45 g, 63%) as an orange foam. *R_f* (CH₂Cl₂–EtOH 20 : 1) 0.55. δ_H (300 MHz; CDCl₃) –0.03, 0.02, 0.06, 0.08, 0.16, 0.20 (12 H, 6 × s, 4 × SiMe), 0.84, 0.86, 0.94 (18 H, 3 × s, 2 × SiC(CH₃)₃), 3.84–3.88 (1 H, m, CH₂-OTBDMS), 4.06 (0.40 H, d, *J* 10.3, C(5)H), 4.23–4.34 (1.60 H, m, C(5)H, CH₂-OTBDMS), 4.84 (0.60 H, s, C(2)H), 4.95 (0.40H, s, C(2)H), 5.03–5.24 (2 H, m, CH₂–C₆H₅), 5.59–5.62 (1 H, m, C(3)H), 7.18–7.37 (5 H, m, C₆H₅CH₂), 7.47–7.53 (2 H, m, Bz), 7.58–7.64 (1 H, m, Bz), 7.90–8.05 (3 H, m, C(6)H, Bz); δ_C (75 MHz; CDCl₃) –5.4, –5.1, –4.9 (3 × q, 4 × SiMe), 17.9, 18.5 (2 × s, 2 × (CH₃)₃C–Si), 25.5, 25.9 (2 × q, 2 × (CH₃)₃C–Si), 57.9, 59.0 (2 × d, C(5)), 60.5, 61.3 (2 × t; CH₂-OTBDMS), 65.2, 65.7 (2 × d, C(2)), 66.7, 67.0 (2 × t, CH₂–C₆H₅), 100.5, 100.7 (2 × d, C(3)), 127.6, 127.8, 127.9, 128.1, 128.3, 128.5, 128.6, 128.9 (8 × d, Bz, C₆H₅CH₂), 132.3 (d, C(6)), 148.4, 148.8 (2 × s, C(4)); *m/z* (FAB⁺) 691.3344 (M⁺ + H. C₃₆H₅₁N₄O₆Si₂ requires 691.3347), 515 (53%), 423 (45%).

(2R,4S,5R)-N-(Benzyloxy)carbonyl-2-[2-(N-benzoylamino)-4-oxo-3,4-dihydropyrimidin-5-yl]-4-hydroxy-5-hydroxymethyl pyrrolidine 6. A solution of HF–pyridine (70% HF, 0.42 cm³, ca. 16 mmol HF) in MeCN (7 cm³) was added dropwise to a solution of **5** (600 mg, 0.87 mmol) in MeCN (18 cm³). After 6 h, the obtained suspension was diluted with AcOH (5 cm³) and evaporated. The residue was suspended in a mixture of AcOH (16 cm³) and MeCN (16 cm³), cooled to –15 °C and NaBH(OAc)₃ (720 mg, 3.40 mmol) was added in portions. After 2 h additional NaBH(OAc)₃ (360 mg, 1.70 mmol) was added in portions. The suspension was slowly warmed to 0 °C and stirred for another 3 h. The mixture was then distributed between EtOAc and H₂O. The organic phase was filtered over celite and evaporated. FC (CH₂Cl₂–EtOH 20 : 3 → 4 : 1) gave compound **6** (322 mg, 79%) as a slightly yellow solid. *R_f*(CH₂Cl₂–EtOH 20 : 3) 0.48. δ_H (300 MHz; CD₃OD) 2.28–2.35 (2 H, m, C(3)H₂), 3.79–4.01 (3 H, m, C(5)H, CH₂OH), 4.39 (1 H, s, C(4)H), 4.88–5.25 (3 H, m, C(2)H, CH₂C₆H₅), 7.16–7.40 (5 H, m, C₆H₅CH₂), 7.58–7.62 (2 H, m, Bz), 7.68–7.83 (2 H, m, C(6)H, Bz), 8.04–8.07 (2 H, m, Bz); δ_C (75 MHz, CD₃OD) 40.1, 40.9 (2 × t, C(3)), 57.3, 58.0 (2 × d, C(2)), 63.1, 63.3 (2 × t, CH₂–OH), 68.5 (t, CH₂C₆H₅), 70.8, 71.3 (2 × d, C(5)), 73.2, 73.5 (2 × d; C(4)), 123.5, 124.2 (2 × s, C(5')), 129.6, 129.1, 129.3, 129.5, 129.7, 130.1, 130.2 (7 × d, Bz, C₆H₅CH₂), 134.1, 134.7 (2 × s, Bz, C₆H₅CH₂), 137.9, 138.1 (2 × d, C(6)); *m/z* (FAB⁺) 465.1773 (M⁺ + H. C₂₄H₂₅N₄O₆ requires 465.1774), 331 (11%), 242 (21%).

(2R,4S,5R)-2-[2-(N-Benzoylamino)-4-oxo-3,4-dihydropyrimidin-5-yl]-4-hydroxy-5-hydroxymethyl pyrrolidine 7. A mixture of **6** (300 mg, 0.65 mmol) and 10% Pd/C (60 mg) in MeOH (24 cm³) was vigorously stirred under an H₂ atmosphere. After 7 h, the solution was filtered over celite and evaporated to give

pyrrolidine **7** (211 mg, 99%) as a white solid. δ_H (300 MHz; CD₃OD) 2.06–2.25 (2 H, m, C(3)H₂), 3.29–3.34 (1 H, m, C(5)H), 3.70–3.75 (2 H, m, CH₂OH), 4.24–4.30 (1 H, m, C(4)H), 4.44–4.50 (1 H, m, C(2)H), 7.53 (2 H, t, *J* 7.0, Bz), 7.61 (1 H, d, *J* 7.0, Bz), 7.91 (1 H, s, C(6)H), 8.05 (2 H, d, *J* 7.4, Bz); δ_C (75 MHz, CD₃OD) 41.2 (t, C(3)), 57.9 (d, C(2)), 63.6 (t, CH₂OH), 70.1 (d, C(5)), 74.4 (d, C(4)), 129.6, 129.9, 130.8, 133.8, 134.5 (5 × d; Bz), 150.5 (d, C(6)); *m/z* (FAB⁺) 331.1406 (M⁺ + H. C₁₆H₁₉N₄O₄ requires 331.1406), 242 (10%), 227 (23%).

(2R,4S,5R)-2-(2-Amino-4-oxo-3,4-dihydropyrimidin-5-yl)-4-hydroxy-5-hydroxymethyl pyrrolidine 8. A solution of **7** (120 mg, 0.36 mmol) in 25% conc. NH₃ (5 cm³) was heated to 60 °C for 18 h. The solution was evaporated to dryness and the residue dissolved in MeOH (3 cm³). The product precipitated after the addition of EtOAc. Filtration and drying under HV gave nucleoside **8** (68 mg, 83%) as a slightly brown powder. δ_H (300 MHz, D₂O) 1.88–1.96 (1 H, m, C(3) H_a), 2.00–2.11 (1 H, m, C(3)H_β), 3.18–3.23 (1 H, m, C(5)H), 3.54–3.67 (2 H, m, CH₂OH), 4.15–4.19 (1 H, m, C(4)H), 4.26 (1 H, dd, *J* 6.6 and 11.0, C(2)H), 7.46 (1 H, s, C(6)H); δ_C (75 MHz, D₂O) 38.4 (t, C(3)), 56.2 (d, C(2)), 61.5 (t, CH₂OH), 67.8 (d, C(5)), 72.6 (d, C(4)), 112.1 (s, C(5')), 148.5 (d, C(6')), 158.9 (s, C(2')), 171.3 (s, C(4')); difference-NOE (500 MHz, D₂O) 1.88–1.96 (C(3)H_a) → 2.00–2.11 (13%, C(3)H_β), 4.26 (1.9%, C(2)H); 2.00–2.11 (C(3)H_β) → 1.88–1.96 (13%, C(3)H_a), 4.15–4.19 (4.7%, C(4)H), 7.46 (1.7%, C(6)H); 3.18–3.23 (C(5)H) → 3.54–3.67 (3.0%, CH₂OH), 4.15–4.19 (1.5%, C(4)H), 4.26 (1.3%, C(2)H); 3.54–3.67 (CH₂OH) → 3.18–3.23 (1.6%, C(5)H), 4.15–4.19 (2.0%, C(4)H); 4.15–4.19 (C(4)H) → 2.00–2.11 (1.6%, C(3)H_β), 3.54–3.67 (1.4%, CH₂OH); 4.26 (C(2)H) → 1.88–1.96 (2.2%, C(3) H_a), 3.18–3.23 (1.5%, C(5)H), 7.46 (2.0%, H–C(6)); 7.46 (H–C(6')) → 2.00–2.11 (1.9%, C(3)H_β), 4.26 (2.0%, C(2)H); *m/z* (ESI[–]) 225.0988 (M[–] – H. C₉H₁₃N₄O₃ requires 225.0987).

(2R,4S,5R)-N-(9-Fluorenylmethoxy)carbonyl-2-[2-(N-benzoylamino)-4-oxo-3,4-dihydropyrimidin-5-yl]-4-hydroxy-5-hydroxymethyl pyrrolidine 9. A solution of *N*-(9-fluorenylmethoxycarbonyloxy)succinimide (440 mg, 1.30 mmol) in THF (6 cm³) was added to a suspension of **7** (218 mg, 0.66 mmol) in dioxane (6 cm³) and 5% aq. NaHCO₃ (8 cm³). After 4 h the solution was evaporated to dryness. Most of the hardly soluble crude product was used in the next step without further purification. A small amount was purified for NMR characterization. It was distributed between EtOAc and H₂O. The organic phase was separated, filtered over celite and evaporated. Product **9** was isolated by FC (toluene–acetone–MeOH 10 : 10 : 1 → 5 : 5 : 1). *R_f* (CH₂Cl₂–EtOH 20 : 3) 0.45. δ_H (300 MHz; (CD₃)₂SO) 1.88–2.21 (2 H, m, C(3)H₂), 3.44–3.76 (3 H, m, C(5)H, CH₂OH), 4.15–4.28 (4 H, m, C(4)H, Fmoc-CH, Fmoc-CH₂), 4.75 (1 H, s, C(2)H), 4.96–5.10 (2 H, m, 2 OH), 7.23–8.08 (14 H, m, C(6)H, Fmoc-H, Bz), 11.87, 12.31 (2 × H, 2 × br s, 2 × NH); *m/z* (FAB⁺) 553.2086 (M⁺ + H. C₃₁H₂₉N₄O₆ requires 553.2087), 179 (79%), 149 (100).

(2R,4S,5R)-N-(9-Fluorenylmethoxy)carbonyl-2-[2-(N-benzoylamino)-4-oxo-3,4-dihydropyrimidin-5-yl]-5-[(4,4'-dimethoxy)triphenylmethyl]-oxymethyl-4-hydroxy pyrrolidine 10. To a suspension of crude **9** (365 mg, 0.66 mmol) in dry pyridine (7 cm³) was added in portions 4,4'-dimethoxytrityl chloride (268 mg, 0.79 mmol). Further additions of 4,4'-dimethoxytrityl chloride every 30 min were added until no starting material was detected by TLC. The solution was diluted with EtOAc, washed with water, dried (MgSO₄) and evaporated. The crude material was purified by FC (CH₂Cl₂–EtOH–NEt₃ 25 : 1 : 0.03 → 20 : 1 : 0.03) to give trityl compound **10** (265 mg, 47% over 2 steps) as a white solid. *R_f* (CH₂Cl₂–EtOH–NEt₃ 20 : 1 : 0.03) 0.47; *m/z*

(ESI⁻) 853.3215 (M⁻ - H, C₅₂H₄₅N₄O₈ requires 853.3237) 631 (7%, M - Fmoc), 283 (44%).

(2S,4R,5S)-N-[(9-Fluorenylmethoxy)carbonyl]-2-[2'-(N-benzoylamino)-4'-oxo-3',4'-dihydropyrimidin-5'-yl]-4-(2'-cyanoethoxy)-(N,N'-diisopropylamino)phosphinoyloxy-5-(4,4'-dimethoxy)triphenylmethyl-oxymethyl pyrrolidine 11. To a solution of **10** (158 mg, 0.18 mmol) in dry THF (5 cm³) was added EtNiPr₂ (158 mm³, 0.92 mmol) followed by 2-cyanoethyl diisopropylchlorophosphoramidite (103 mm³, 0.46 mmol). After 1 h, H₂O was added and the product extracted twice with EtOAc. The combined organic layers were dried (MgSO₄) and evaporated. FC (CH₂Cl₂-EtOH-NEt₃, 50: 1: 0.03 → 40: 1: 0.03) gave phosphoramidite **11** (172 mg, 88%) as a white foam. R_f(CH₂Cl₂-EtOH-NEt₃, 30: 1: 0.03) 0.30, 0.36; δ_p (161.9 MHz; CDCl₃) 151.04, 151.49; m/z (ESI⁻) 1053.4290 (M⁻ - H, C₆₁H₆₂N₆O₉P requires 1053.4316).

Synthesis of oligonucleotides

All oligomers were synthesized on a 1.0 or 1.3 μm scale on an Applied Biosystems Expedite 8900 or a Pharmacia LKB Gene Assembler Special DNA synthesizer, using standard phosphoramidite chemistry. Natural phosphoramidites were purchased from Glen Research. The pyrrolidino phosphoramidites were prepared as described. The 2'-deoxypseudoisocytidine phosphoramidite was prepared as described previously.¹⁰ As starting units, commercially available natural nucleosides bound to CPG-solid support were chosen. The standard synthetic procedure was used with minor modifications. The coupling time was extended from 1.5 to 6 min for the modified monomers. Coupling efficiencies were >97% as determined by trityl assay with (*S*-benzylthio)-1*H*-tetrazole (0.25 M in CH₃CN) instead of tetrazole as activator. After synthesis, the oligonucleotides were cleaved from the solid support and deprotected in conc. NH₃ at rt or 55 °C. The crude oligonucleotides were purified by ion exchange-HPLC and desalted over Sep-Pak C-18 cartridges (Waters) and were obtained in yields of 17–42% (OD 260 nm). The purity of the oligomers was confirmed to be >95% by RP-HPLC and their structural integrity, especially the cleavage of the Fmoc- and benzoyl-protecting groups, was proven by electrospray mass spectrometry. The difference between the calculated and the measured mass was always <0.05%.

UV-melting curves

UV-melting curves were measured on a Varian Cary 3E UV/Vis spectrophotometer and monitored at 260 nm. A heating-cooling-heating cycle in the temperature range 20–90 °C or 0–90 °C was applied, with a linear gradient of 0.5 °C min⁻¹. While the heating cycles were superimposable, the cooling cycles usually showed slight hysteresis for the association of the third strands. *T_m* values were defined as the maximum of the first derivative of the melting curves (heating ramp) using the Varian WinUV or Microcal Origin softwares. For temperatures <20 °C, nitrogen was passed through the spectrophotometer to avoid condensation on the cuvettes. To avoid evaporation of the solutions, 6–8 drops of dimethylpolysiloxane were added on top of the samples in the cell. Oligonucleotides were mixed in stoichiometric amounts by using the UV extinction coefficients of natural oligonucleotides. The buffer (140 mM KCl, 7 mM NaH₂PO₄, 0.5 mM MgCl₂) was chosen to approximate the intracellular cationic environment as closely as possible.

Circular dichroism spectra

CD-spectra were recorded on a Jasco J-715 spectropolarimeter equipped with a Jasco PFO-350S temperature controller. The temperature was measured directly in the sample. The strand concentration was 1.2 μM in 140 mM KCl, 7 mM NaH₂PO₄, 0.5 mM MgCl₂ at pH 6. The samples were scanned at a speed of 50 nm min⁻¹, band width of 1 nm, response of 1 sec and in a 210–320 nm range at constant temperature. Each spectrum was taken as an average of three scans using a 10 mm cell. Subsequently, the graphs were smoothed with a noise filter. For the temperature scan, the spectra were measured at 217 nm between 10 and 80 °C with a resolution step of 0.1 °C and a slope of 50 °C h⁻¹.

Gel retardation experiments

Non-denaturing 20% polyacrylamide gel were prepared with a 19: 1 acrylamide to bisacrylamide ratio. The gel and the buffer contained TBM (90 mM Tris, 90 mM boric acid, 10 mM MgCl₂, pH 7.1). After conditioning of the gel (1 h at 120 V) and annealing of the oligonucleotides, the samples were loaded onto the gel (loading buffer) and electrophoresis was performed at 120 V for 18 h at 4 °C. Bands were detected by UV shadowing on a TLC plate at 254 nm.

Acknowledgements

The authors would like to thank the Swiss National Science Foundation for financial support of this project. Thanks also goes to Dr Sabrina Buchini for precious help with gel electrophoresis.

References

- (a) D. Praseuth, A. L. Guieysse and C. Hélène, *Biochim. Biophys. Acta*, 1999, **1489**, 181–206; (b) R. V. Guntaka, B. R. Varma and K. T. Weber, *Int. J. Biochem. Cell Biol.*, 2003, **35**, 22–31; (c) M. M. Seidman and P. M. Glazer, *J. Clin. Invest.*, 2003, **112**, 487–494.
- (a) S. Buchini and C. J. Leumann, *Curr. Opin. Chem. Biol.*, 2003, **7**, 717–726; (b) K. R. Fox, *Curr. Med. Chem.*, 2000, **7**, 17–37.
- (a) S. Obika, T. Uneda, T. Sugimoto, D. Nanbu, T. Minami, T. Doi and T. Imanishi, *Bioorg. Med. Chem.*, 2001, **9**, 1001–1011; (b) T. Imanishi and S. Obika, *Chem. Commun.*, 2002, 1653–1659; (c) M. Koizumi, K. Morita, M. Daigo, S. Tsutsumi, K. Abe, S. Obika and T. Imanishi, *Nucleic Acids Res.*, 2003, **31**, 3267–3273; (d) D. Renneberg and C. J. Leumann, *ChemBioChem*, 2004, **5**, 1114–1118.
- (a) I. Prévot-Halter and C. J. Leumann, *Bioorg. Med. Chem. Lett.*, 1999, **9**, 2657–2660; (b) S. Obika, Y. Hari, M. Sekiguchi and T. Imanishi, *Chem. Eur. J.*, 2002, **8**, 4796–4802; (c) S. Buchini and C. J. Leumann, *Angew. Chem., Int. Ed.*, 2004, **43**, 3925–3928.
- (a) B. Cuenoud, F. Casset, D. Hüsken, F. Natt, R. M. Wolf, K.-H. Altmann, P. Martin and H. E. Moser, *Angew. Chem., Int. Ed.*, 1998, **37**, 1288–1291; (b) M. J. J. Blommers, F. Natt, W. Jahnke and B. Cuenoud, *Biochemistry*, 1998, **37**, 17714–17725; (c) M. Sollogoub, R. A. J. Darby, B. Cuenoud, T. Brown and K. R. Fox, *Biochemistry*, 2002, **41**, 7224–7231; (d) V. Roig and U. Asseline, *J. Am. Chem. Soc.*, 2003, **125**, 4416–4417.
- S. Rhee, Z.-J. Han, K. Liu, H. T. Miles and D. R. Davies, *Biochemistry*, 1999, **38**, 16810–16815.
- A. Häberli and C. J. Leumann, *Org. Lett.*, 2001, **3**, 489–492.
- A. Häberli and C. J. Leumann, *Org. Lett.*, 2002, **4**, 3275–3278.
- A. Häberli, A. Mayer and C. J. Leumann, *Nucleosides, Nucleotides Nucleic Acids*, 2003, **22**, 1187–1189.
- A. Mayer and C. J. Leumann, *Nucleosides, Nucleotides Nucleic Acids*, 2003, **22**, 1919–1925.
- (a) J. Bijapur, M. D. Keppler, S. Bergqvist, T. Brown and K. R. Fox, *Nucleic Acids Res.*, 1999, **27**, 1802–1809; (b) K. G. Rajeev, V. R. Jadhav and K. N. Ganesh, *Nucleic Acids Res.*, 1997, **25**, 4187–4193.
- J. M. Dagle and D. L. Weeks, *Nucleic Acids Res.*, 1996, **24**, 2143–2149.